Available online at www.sciencedirect.com

SCIENCE DIRECT®

Hearing Research 193 (2004) 111–120

HEARING RESEARCH

www.elsevier.com/locate/heares

Separating stimulus-locked and unlocked components of the auditory event-related potential

Dennis J. McFarland [a,*], Anthony T. Cacace [b]

[a] *Laboratory of Nervous System Disorders, The Wadsworth Center, NYS Department of Health, P.O. Box 509, Empire State Plaza, Albany, NY 12201-0509, USA*

[b] *Department of Neurology, The Neurosciences Institute, Albany Medical College, Albany, NY, USA*

Abstract

A new method is evaluated for separating stimulus-locked and unlocked components of auditory event-related EEG activity. The new method uses a regression based subtraction procedure as a way to account for latency and amplitude variability within individual trials. It was applied using the oddball paradigm under conditions of active and passive listening and analyzed as spectral correlations (normalized differences) between post-stimulus epochs of standard, target or deviant stimulus conditions and silent pre-stimulus baseline activity.

The regression-subtraction procedure accounted for a greater amount of variance than a method that uses linear subtraction alone. The major component of the response to auditory stimulation was an event-related synchronization in the delta and theta (2–4 Hz) frequency range. Event-related desynchronizations were also observed in the 10 Hz (alpha/mu) and in the 20–30 Hz (beta) frequency range.

The regression based subtraction procedure provides better separation of stimulus-locked and unlocked components of event-related EEG activity then linear subtraction alone. Stimulus-locked and unlocked components show different patterns and topographies of effects related to attention and active discrimination. Studying both stimulus-locked and unlocked components of event-related EEG reactivity in the frequency domain provides a more comprehensive account of dynamic brain activity subserving auditory information processing.

Keywords: Event-related potentials; Event-related synchronization; Event-related desynchronization; Phase; Spectral dynamics

1. Introduction

Electroencephalographic activity (EEG) is a complex and dynamic signal that is reactive to sensory, perceptual, and cognitive processes. How best to analyze the multifaceted nature of this signal and extract maximal information is an unsettled question and a matter of ongoing debate. This conundrum is due in large part to the fact that a comprehensive model of event-related processes has yet to be elucidated. From a historical perspective, use of signal averaging in the time domain is probably the most common strategy for extracting event-related information (Dawson, 1951, 1954). The basic premise underlying this approach assumes that data contained within individual trials is composed of a linear combination of stimulus-locked activity and background noise. In theory, by averaging many post-stimulus epochs of EEG to suprathreshold stimuli, the noise component decreases toward zero and the stimulus or event locked component (also called event-related potential, ERP) emerges from the recording. The signal-to-noise ratio of the stimulus-locked component is improved by the square root of the number of post-stimulus epochs averaged. These general assumptions have evolved into the so-called “*additive model*” where extraction of stimulus-locked activity is based exclusively on time domain analyses.

One fundamental shortcoming of the additive model concerns the way in which non-stimulus-locked EEG activity is handled (Klimesch et al., 1998).

---

[*] Corresponding author. Tel.: +1-518-473-4680; fax: +1-518-486-4910.

E-mail address: mcfarlan@wadsworth.org (D.J. McFarland).

0378-5955/$ - see front matter © 2004 Elsevier B.V. All rights reserved.
doi:10.1016/j.heares.2004.03.014

Non-stimulus-locked activity includes EEG that is *reactive* to the stimulus, but not locked to the event (also called induced or emergent; e.g., Bullock, 1992; Ohl et al., 2003) and unwanted noise. On purely phenomenological grounds, we favor the term "*unlocked*" to describe the reactive component of the EEG spectra that is not locked to the stimulus or event. In the additive model, unlocked activity is treated as noise. As a result, unlocked activity goes undetected because it is eliminated from the average by phase cancellation. This state-of-affairs is problematic, since unlocked EEG activity is potentially a rich source of information about brain function (Başar and Bullock, 1992). Therefore, alternative conceptualizations and better signal processing strategies are needed to minimize this loss of information and avoid potentially compromised interpretations. Furthermore, if components-of-interest contain substantial trial-to-trial variability in latency and amplitude, then use of signal averaging in the time domain will not be an effective approach for extracting pertinent event-related information (e.g., Lange et al., 1997; Truccolo et al., 2002).

Methods to extract co-existent stimulus-locked and unlocked event-related EEG activity could enhance understanding of neural information processing and provide a more comprehensive account of brain dynamics underlying sensory and cognitive events (e.g., Pfurtscheller and Lopes da Silva, 1999; Bastiaansen and Hagoort, 2003). A novel signal processing strategy was proposed by Kalcher and Pfurtscheller (1995) for extracting event-related unlocked EEG activity. Their method involves subtracting the stimulus-locked component (i.e., the averaged ERP) from individual trials of EEG. Once stimulus-locked activity is removed, the residual or unlocked component becomes available for further analysis. With this method, post-subtracted unlocked activity is further quantified by filtering EEG into specific passbands, converting voltage to power, averaging over individual trials, and transforming data to a percentage scale referenced to a pre-stimulus baseline. By referencing post-stimulus epochs to a pre-stimulus baseline, event-related synchronization (ERS; increased power) and event-related desynchronization (ERD; decreased power) of EEG activity could be assessed as a function of frequency (Pfurtscheller and Lopes da Silva, 1999). However, a primary issue-of-contention concerns limitations of the linear subtraction procedure, since it does not account for latency and amplitude variability of the stimulus-locked component within individual trials (Lange et al., 1997). As a result, applying this procedure might remove too little or too much activity and potentially have a negative impact on other quantitative analyses (Truccolo et al., 2001).

To address this issue and to evaluate unlocked activity, we compared the method proposed by Kalcher and Pfurtscheller (1995) with a variation and extension of this technique, which attempts to account for latency and amplitude variability in the data. This new method was designed with the intent of estimating the amplitude and position of the waveform to be subtracted from individual trials by a regression procedure using a sliding time window with varying degrees of lag. This method is conceptually similar to latency-corrected averaging (Woody, 1967) and involves latency-corrected subtraction of the averaged waveform from individual trials. The Kalcher and Pfurtscheller (1995) model assumes constant amplitude and latency of stimulus-locked activity within individual trials. We chose to evaluate this method with a relatively simple model, that accounts for amplitude and latency variability on the entire waveform. We used the oddball paradigm under active and passive listening conditions to compare these two methods and to examine the contributions of stimulus-locked and unlocked EEG activity. Advantages of the oddball paradigm for assessing these effects include ease of application, use of simple instructions, and extensive neurophysiological background research that has focused on various sensory, perceptual, and cognitive processes (e.g., Näätänen, 1992, 2003; Donchin and Coles, 1988; Polich and Herbst, 2000). We hypothesize that the regression-subtraction method would allow for better separation of stimulus-locked and unlocked EEG activity than linear subtraction alone.

Additionally, more complex models are possible, such that each component (e.g., N100, P300) is modeled with variable amplitude and latency variability (Lange et al., 1997). However, there are problems with the use of complex models, such as selecting the number of components to model and handling the overlap of simultaneously active sources. We initially examined broad-banded spectra and subsequently focused on four frequency bands (2, 4, 10 and 20 Hz) where ERS and ERD effects were especially prominent. Selection of these specific frequencies was based in part on the current results as well as other reference data obtained from a more comprehensive topographical study using similar methods (Cacace and McFarland, 2003).

2. Methods

2.1. Participants

Ten adults (4 males; 6 females) ranging in age from 24 to 53 years (mean age, 39 years) with negative histories of neurologic and otologic problems (pure tone thresholds <25 dB HL, 0.25–4.0 kHz bilaterally) participated. All individuals were briefed as to the nature of the experiment and provided signed informed consent. The Internal Review Board (IRB) of the Albany Medical College approved the study.

2.2. Data acquisition

Electroencephalographic activity was recorded from five scalp locations (Fz, Cz, Pz, C3, C4) based on the 10–20 system of the International Federation. Electrodes were referenced to a non-cephalic sterno-vertebral site and grounded to the left forearm. Two additional bipolar channels were used for monitoring vertical and horizontal electro-ocular (EOC) activity (i.e., eye blinks and lateral eye movements). These channels were included so that EEG contaminated with high levels of EOC could be removed from the average prior to data analysis. Electroencephalographic activity was collected and stored in digital form on a trial-by-trial basis using commercially available hardware and software (SCAN and STIM systems, NeuroScan Inc., El Paso, TX, USA). Signal processing (i.e., time domain averaging, autoregressive spectral analysis, etc.) was performed offline with custom software.

Individuals were tested in a lighted, commercially constructed sound attenuating test booth (Tracoustics, RE-145) and were seated on a padded chair with head, leg and arm support. Participants were instructed to remain awake and focus on a designated point on a wall looking straight ahead. They were also asked to minimize any unnecessary eye movements, body movements and/or muscle contractions during testing. Electroencephalographic activity was collected over a 2000 ms time epoch (1000 ms silent pre-stimulus silent baseline interval; 1000 ms post-stimulus recording interval), amplified 20,000×, filtered between 0.1 and 100 Hz (12 dB/octave slope; Grass model 12, Neurodata Acquisition System) and digitized at 256 Hz with 16-bit resolution. Triggering for EEG data acquisition, analog-to-digital conversion, and stimulus presentation were performed by STIM and SCAN systems. Individual trials of EEG activity exceeding 50 μV were rejected as artifacts and were not included in the data analysis.

2.3. Experimental task

An oddball paradigm was used whereby sequential standard and oddball (target/deviant) auditory stimuli were presented with different probabilities. Depending on task demands, either active discrimination of the target (attend condition) or passive listening to the deviant (no-attend condition) was required. In the attend condition, individuals were instructed to press a button as quickly as possible on an instrument panel with the index finger of their right hand (STIM system response pad, P/N 1141) every time the target stimulus was discriminated from the stream of frequently occurring standards. In the no-attend passive listening condition, neither button press nor silent counting was required for detecting the deviant.

2.4. Stimuli

Standard stimuli were 250 Hz pure tones 50 ms in duration and windowed by a Blackman function having 5 ms rise/fall times. Oddballs (target and deviant) stimuli were presented at +6 just noticeable frequency (JNDs) above their frequency discrimination threshold for 250 Hz (see Cacace and McFarland, 2003 for details regarding the psychophysical assessment). Presenting oddballs at +6 JNDs above the frequency discrimination threshold insures that individual participants could easily distinguish the oddballs from the stream of frequently occurring standards. The averaged psychometric function showing frequency discrimination performance for the group of subjects is shown in Fig. 1. The dashed line extending from the y to x-axis represents the frequency discrimination threshold corresponding to 1 JND (i.e., 70% correct performance for a 3-IFC task). From Fig. 1 it can be seen that when frequency differences were 64 Hz, discrimination performance was at 100% for all participants. Therefore, stimulus selection at +6 JNDs above discrimination threshold was adequate to insure a relatively simple target detection task for individual participants.

Four blocks of each active and passive stimulus condition were collected (eight blocks total; probability of the standard, 0.8; probability of the target/deviant, 0.2; total trials within individual blocks, 240). Stimuli were presented binaurally at a level approximating 80 dB SPL through insert earphones (Etymotic-ER3A) and

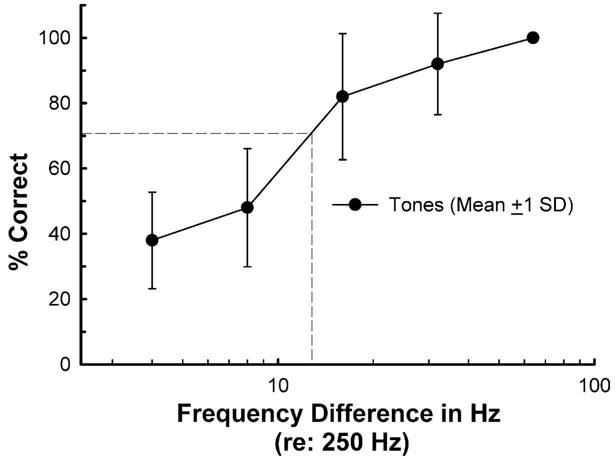

Fig. 1. Psychophysical function representing percent correct performance (y-axis) versus change in frequency (x-axis). Data were obtained with a three interval forced choice (3-IFC) oddity paradigm. Filled circles represent mean values, error bars are 1 standard deviation (SD) above and below the mean. The dashed line represents the frequency discrimination threshold at the 70% correct for the 3-IFC task. Frequency discrimination thresholds or just noticeable differences were obtained individually for each participant prior to data collection. Data were obtained using a block-randomized design, where 10 stimuli were presented at each of five frequency differences of 4, 8, 16, 32, and 64 Hz. The base frequency was 250 Hz.

pseudo-random interstimulus intervals (2.5 ± 0.25 s) were used. The experimental conditions were presented to each participant in a different random order.

2.5. Signal processing

Broadband spectral analysis was performed with a 40th order autoregressive (AR) model. Mean and linear trends were removed from each epoch, and then AR coefficients were estimated using the Burg algorithm (Press et al., 1988). For each trial, point-biserial correlations between a variable reflecting the presence or absence of the stimulus and the spectral bins of the EEG were computed separately for the pre-stimulus baseline and post-stimulus response intervals. Because Pearson's *r* represents a normalized difference metric that is signed, direct comparison between stimulus conditions is possible because the metric is scale independent. In the computations reported herein, Pearson's *r* was computed between the spectral bin for each data segment and a dummy variable representing the presence (1 for post-stimulus interval) or absence (−1 for pre-stimulus interval) of the stimulus during that interval.

Power spectra and Pearson's *r* spectra were computed from uncorrected epochs of EEG as well as from epochs of EEG with an estimate of the stimulus-locked component removed. The first procedure used for removing the stimulus-locked component followed the method described by Kalcher and Pfurtscheller (1995). This approach involved subtracting the average from individual epochs of EEG on a trial-by-trial basis. In the new procedure, spectra were computed from individual trials in which the average response was removed via a latency-corrected subtraction of the average, henceforth termed regression-subtraction procedure. Specifically, EEG activity from each trial first had the averaged waveform regressed according to Eq. (1) over a sliding time window to determine the time point that produced the largest regression coefficient. Then, the averaged value weighted by the regression coefficient was subtracted from each individual epoch at the point where the regression coefficient was maximal. The mathematical expression describing this approach is provided below:

$$b_\tau = \sum_{t=0}^{T} f(t) * g(t+\tau), \tag{1}$$

where b is the regression coefficient; $f(t)$ is the average ERP template; τ is the jitter; $g(t+\tau)$ is the single trial epoch; and T is the epoch length. Since the maximum value of τ was 100 ms, the value of T was 900 ms for all analyses. The samples were truncated at the lead end of the baseline and at the trailing end of the post-stimulus epoch. We compared uncorrected spectra, spectra corrected for the average (after Kalcher and Pfurtscheller, 1995) and latency-corrected subtraction with lags of 0 ms (i.e., no lag), ±25, ±50 and ±100 ms.

2.6. Statistical analysis

A five-way repeated measures analysis-of-variance (ANOVA) was used to evaluate for the effects of condition (active vs. passive listening), electrode location (Fz, Cz, Pz), stimulus type (standard vs. oddball [target/deviant]) frequency bands (centered at 2, 4, 10 and 20 Hz) and method (uncorrected, linear subtraction, regression-subtraction [0 ms lag, ±25 ms lag, ±50 ms lag, and ±100 ms lag]). In this analysis, Pearson's *r*-values were used as the dependent variable and data were collapsed across four separate attend and no-attend conditions to optimize signal-to-noise ratio.

3. Results

Examples of EEG spectra averaged across subjects for active and passive listening conditions are shown in Figs. 2 and 3 for the Pz electrode site. In the active listening condition (Fig. 2, attend), columns 1 and 2 compare stimulus and baseline conditions for standard and target stimuli; in the passive listening condition (Fig. 3, no-attend) columns 1 and 2 compare stimulus and baseline conditions for standard and deviant stimuli. In both figures, column 3 represents Pearson's *r* spectra computed for each spectral bin between the post-stimulus interval and pre-stimulus baseline interval for standard (solid line) and target or deviant stimulus conditions (dotted line), respectively. In these plots, positive correlations represent ERS of EEG activity and negative correlations represent ERD of EEG activity. The first row of plots correspond to raw uncorrected data; the subsequent four rows correspond to changes in EEG spectra after the average was removed from individual trials by either linear subtraction or by the regression-subtraction procedure described previously.

3.1. On-going background EEG

In the spectral plots shown in Figs. 2 and 3 (columns 1 and 2), silent pre-stimulus baseline activity has the characteristic features of EEG spectra recorded from the scalp. Using the central electrode site (Pz) as an example, energy is concentrated in lower frequency regions with prominent peaks centered at ∼4 and ∼10 Hz. Above this frequency, a relatively rapid fall-off of energy occurs.

3.2. Attend condition

Results from the active listening condition show that EEG is reactive to the acoustic input stimulus and is modulated by attentional processes in a frequency specific manner (i.e., the increase in voltage is generally below 7 Hz). In comparison to pre-stimulus baseline

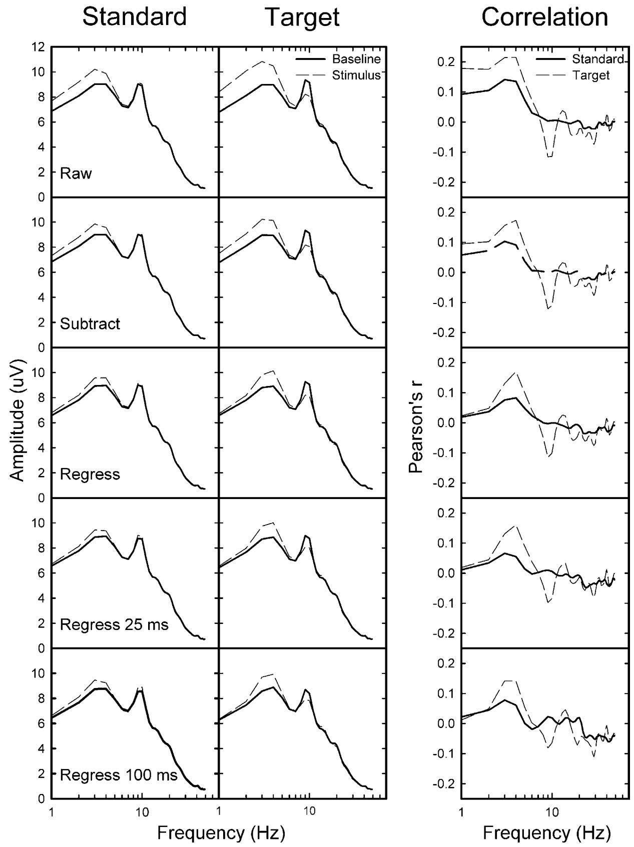

Fig. 2. Averaged spectra ($n = 10$) in the active listening attend condition are shown. Columns 1 and 2 compare stimulus (dotted lines) and baseline conditions (solid lines) for standard and target stimuli. Column 3 represents Pearson's r spectra between the post-stimulus interval and pre-stimulus baseline for standard (solid line) and target conditions (dotted lines). Positive correlations represent ERS effects; negative correlations represent ERD effects as a function of frequency. The first row corresponds to raw uncorrected data; the subsequent four rows correspond to changes in EEG spectra after the composite average was removed from individual trials either by linear subtraction or by one of the regression-subtraction procedures.

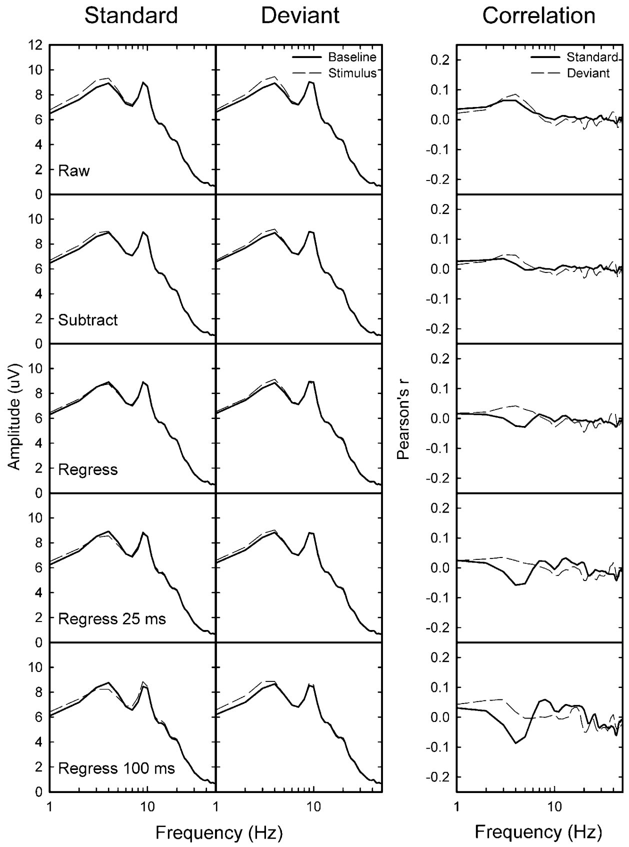

Fig. 3. Averaged spectra ($n = 10$) in the passive listening no-attend condition are shown. Columns 1 and 2 compare stimulus (dotted lines) and baseline conditions (solid lines) for standard and target stimuli. Column 3 represents Pearson's r spectra between the poststimulus interval and pre-stimulus baseline for standard (solid line) and target conditions (dotted lines). Positive correlations represent ERS effects; negative correlations represent ERD effects as a function of frequency. The first row corresponds to raw uncorrected data; the subsequent four rows correspond to changes in EEG spectra after the composite average was removed from individual trials either by linear subtraction or by one of the regression-subtraction procedures.

activity, event-related changes in EEG spectra were largest in approximately the 1–4 Hz region and in attention related target conditions (columns 1 and 2, Fig. 2). Additionally, more complex frequency dependent ERS and ERD effects were evident in the correlation plots (column 3). Event-related synchronization effects were most prominent in the frequency band centered at ~4 Hz, although there was an electrode dependent spread of synchronization down to 1 Hz. Event-related desynchronization effects occurred in higher frequency bands, most notably at ~10 and also within the 20–30 Hz range. This dynamic pattern of event-related EEG reactivity occurred in the power spectra of both the raw uncorrected data and in correlation data after the stimulus-locked component was removed from individual trials. Whereas the linear subtraction procedure produced a reduction in energy predominantly at low frequencies and in the target condition, ERS effects at 4 Hz and ERD effects at 10 and in the 20–30 Hz range were largely unaffected. The regression-subtraction procedure at various time lags further reduced low frequency energy. These findings suggest that frequency dependent changes in EEG reactivity were contained predominantly within the *unlocked* component. Indeed, such effects would go undetected with the commonly used time domain signal averaging strategy.

3.3. No-attend condition

In the passive listening condition (Fig. 3), low frequency EEG activity was also reactive to standard and deviant stimuli. However, in comparison to the attend condition (Fig. 2), the response in the low frequency range was clearly reduced under both standard and deviant stimulus conditions. In the correlation plots (column 3), there was also a corresponding reduction in magnitude of the ERS. Significantly, ERD effects to the deviant were *absent*. Both the linear subtraction and the regression-subtraction procedure primarily reduced EEG activity in the lower frequency range.

3.4. Statistical analysis

The ANOVA with repeated measures showed significant main effects for condition ($F = 14.38$, $p < 0.0043$), location ($F = 3.94$), $p < 0.0381$), method ($F = 5.89$, $p < 0.0003$), and frequency band ($F = 12.10$, $p < 0.0001$). There were significant interactions between location × method ($F = 4.16$, $p < 0.0001$), condition × frequency band ($F = 11.53$, $p < 0.0001$), location × frequency band ($F = 3.45$, $p < 0.0059$), stimulus × frequency band ($F = 11.62$, $p < 0.0001$), method × frequency band ($F = 7.08$, $p < 0.0001$), condition × location × frequency band ($F = 2.92$, $p < 0.0155$), condition × method × frequency band ($F = 2.64$, $p < 0.0016$), ($F = 2.64$, $p < 0.0016$), location × stimulus × frequency band ($F = 4.64$, $p < 0.0007$), location × method × frequency band ($F = 6.12$, $p < 0.0001$), location × stimulus × method × frequency band ($F = 1.52$, $p < 0.0452$) and condition × location × stimulus × method × frequency band ($F = 1.96$, $p < 0.0027$). Thus, all of the variables in the analysis produced significant effects. However, as indicated by the significant interactions, the effects observed were complex and not simply additive.

The effects of task and analysis method are perhaps most complex for the 4 Hz bin. These effects are summarized in Fig. 4, averaged over attend/no-attend conditions. In this figure, it can be seen that stimulus presentation resulted in a generalized synchronization of EEG activity, which produced effects that were greater for oddball than standard stimuli. Most evident were the effects of method, depicted separately on the *x*-axis of the graph. Specifically, the procedures designed to remove the stimulus-locked component produced increasing reductions in synchronized activity as amplitude variability and greater degrees of the temporal variability in the waveforms were taken into account. The residual unlocked activity was best elucidated following the regression-subtraction procedure with the sliding time window and ±25 or ±100 ms lag times. Focusing on the sliding time window with the ±100 ms lag time, it can be seen that synchronized activity was all but absent in the response to the standard at central and posterior sites (Cz and Pz), but a substantial unlocked component was present for the standard at Fz. Significantly, the unlocked component was dominant for oddball conditions in a graded manner from anterior (Fz) to posterior sites (Pz).

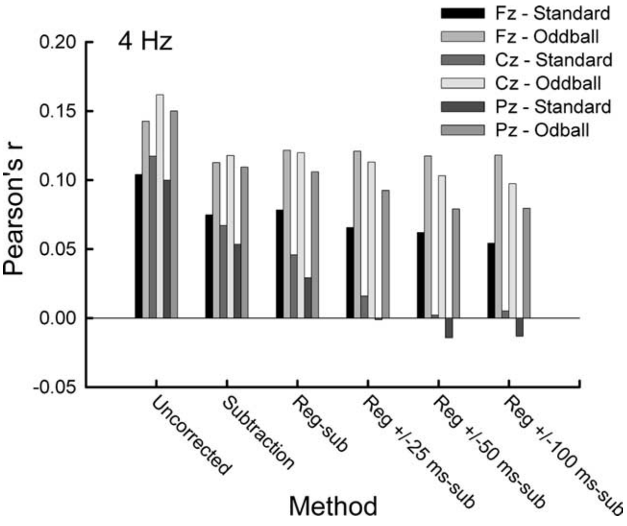

Fig. 4. Bar graphs plotting a three-way location × stimulus × method interaction for the 4 Hz data, derived from ANOVA. Data are collapsed across condition. The *y*-axis represents Pearson's *r* correlation coefficients and *x*-axis represents the method for removing the stimulus-locked component. The first category (raw uncorrected data) was used as a point-of-reference. The parameters of the graph are each of three central electrode sites for standard and oddball stimuli.

3.5. Comparison of stimulus-locked and unlocked components

The size of the stimulus-locked and unlocked components was estimated by considering the results of the regression-subtraction procedure using the sliding time window at the ±100 ms lag time. In this comparison, the unlocked component was derived by the regression-subtraction procedure. The unlocked component was subtracted from the total spectra to derive the stimulus-locked component. These comparisons are presented in Figs. 5 (attend condition) and 6 (no-attend condition). For data in the attend condition shown in Fig. 5, column 1 represents the total *r* spectra for standard and target conditions at each of three central electrode sites. Column 2 shows the unlocked component derived by the regression-subtraction procedure at ±100 ms lag. The unlocked component consists of a prominent 4 Hz ERS that is greater for target than standard conditions; ERDs at 10 and in the 20–30 Hz range are also observed. The stimulus-locked component under standard and target conditions (Column 3) consists mainly of synchronized low frequency energy below 7 Hz. The magnitude of the ERS is maximum for the target at 1 Hz and is most prominent at the posterior electrode site Pz. For data in the no-attend condition shown in Fig. 6, column 1, total *r* spectra shows substantially reduced ERS in the low frequencies. Significantly, ERDs were absent. In the unlocked component, a prominent ERD is observed at 4 Hz in response to the standard, whereas the stimulus-locked component shows a prominent ERS

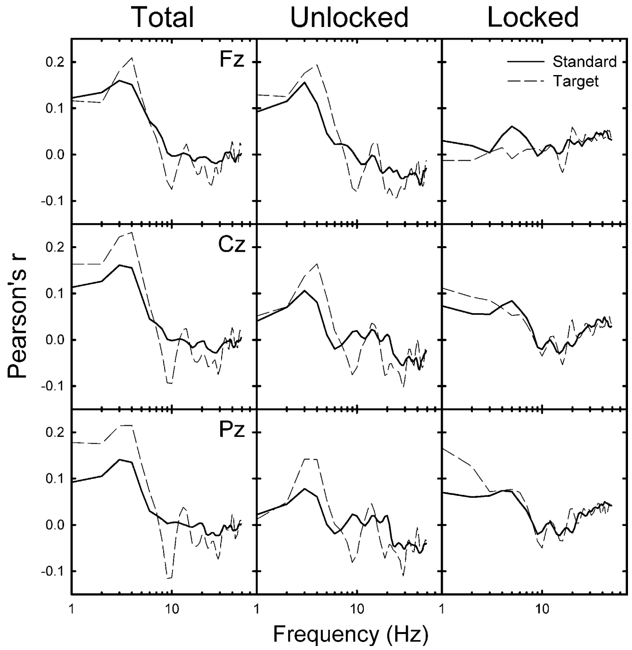

Fig. 5. Average spectra of r-values in the active listening condition. Column 1 displays raw spectra for the standard (solid line) and target (dotted line). Column 2 shows the unlocked component obtained by the regression-subtraction procedure allowing up to 100 ms lag. Column 3 shows the stimulus-locked component obtained by subtracting column 2 data from the total spectra (column 1).

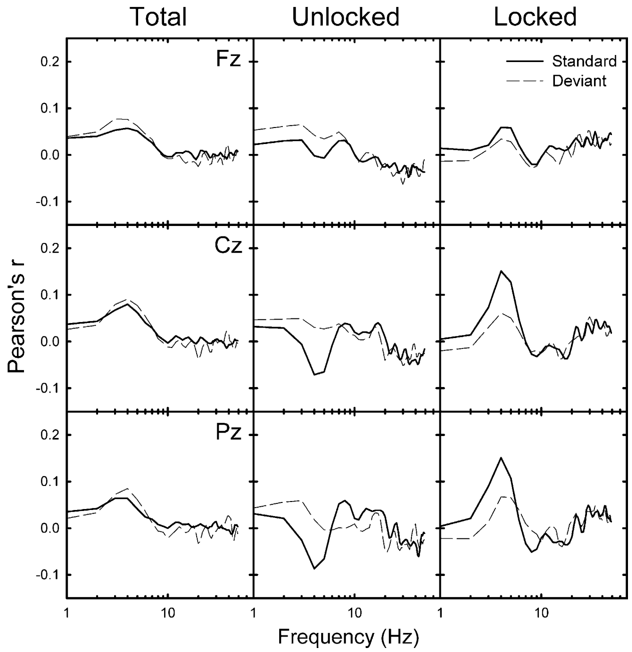

Fig. 6. Average spectra of r-values in the passive listening condition. Column 1 displays raw spectra for the standard (solid line) and target (dotted line). Column 2 shows the unlocked component obtained by the regression-subtraction procedure allowing up to 100 ms lag. Column 3 shows the stimulus-locked component obtained by subtracting column 2 data from the total spectra (column 1).

at the same corresponding frequency, although opposite in sign. These reciprocal effects on unlocked and stimulus-locked components are consistent with phase resetting of the background oscillations. Indeed, such effects are largely absent in the response to the deviant stimulus.

4. Discussion

Use of the oddball paradigm in active discrimination and passive listening conditions resulted in dynamic frequency dependent changes in EEG spectra. When we consider these dynamic modulations in brain activity, including ERS and ERD effects, it is important to keep in mind that they represent only a small proportion of the variance in relation to the total on-going background (baseline) EEG (r^2, less than 5%). On a percentage basis, the order of magnitude of these effects are similar to those changes observed in event related or block designed functional magnetic resonance (*f*MRI) studies to sensory stimulation or cognitive challenges based on blood oxygenation level dependent (BOLD) signals (e.g., Buckner and Braver, 1999; Melcher et al., 1999). We emphasize that in both EEG and *f*MRI studies, the magnitude of these event-related effects are baseline dependent.

In comparison to the pre-stimulus baseline, event-related reactivity observed in the total EEG spectra was characterized by a modulation (increased voltage) below ~7 Hz. This activity is further enhanced during conditions requiring attention to, and discrimination of the target. The correlated EEG activity shows further structural complexities in the event-related spectra. Specifically, prominent ERS effects were observed at ~4 Hz whereas ERD effects dominated in the higher frequencies (10 and 20–30 Hz). When the stimulus-locked component was removed from individual trials, most notably by the regression-subtraction procedure allowing ±25 to ±100 ms lag times, a substantial amount of residual energy was found to be reactive but not locked to stimulus or task conditions. Indeed, the majority of unlocked energy was primarily localized within target and standard stimulus conditions where attention and active discrimination (cognitive processing) was required. The traditional time-domain approach (e.g., Dawson, 1951, 1954) treats this unlocked energy as noise. Delineating unlocked activity from background noise can also be a concern. However, the unlocked component is frequency dependent and shows stimulus and task specific reactivity, whereas non-EEG noise (including electromyographic activity, see Goncharova et al., 2003) is broadband and non-reactive to the input. These considerations further reinforce the use of broadband spectral analysis (Cacace and McFarland, 2003) in contrast to approaches using relatively narrow band-pass filters when processing event-related EEG. Our discussion now focuses on improvements in methodology for isolating event-related non-phase-locked activity from background EEG, including the direct comparisons between unlocked and stimulus-locked activity.

4.1. Removing the stimulus-locked component from individual trials

In our analysis, the more complex regression-subtraction procedure using a sliding window with time lags in the ±25 to ±100 ms range appears to model the phase-locked component better than the linear subtraction procedure proposed by Kalcher and Pfurtscheller (1995). This occurs because the sliding regression captures the trial-to-trial variation in latency and amplitude of the stimulus-locked component; linear subtraction alone is insensitive to these factors. This is evident for attended targets in the 1–2 Hz range and for 4 Hz responses to unattended standards. Indeed, the regression-subtraction procedure operated best in a time frame where variability of ERPs (~100–1000 ms range) was maximal (Nishida et al., 1997). Another novel feature of the present study is the direct comparison of stimulus-locked and unlocked components. Whereas others have used the subtraction procedure to remove stimulus-locked components and have compared this to the total raw data, they have *not* compared the residual component with that which was removed (e.g., Kalcher and Pfurtscheller, 1995; Klimesch et al., 1998). The direct comparison of stimulus-locked and unlocked components allows for a determination of whether or not this activity reflects the same or different underlying processes. Although limited in spatial resolution, the present study shows that stimulus-locked and unlocked components have differing reactivities at different electrode locations. This implies that different underlying processes are contributing to these effects.

One potential problem with the latency-corrected average technique of Woody (1967) is that the template may "*lock on* " to some feature in the EEG other than stimulus or event-related activity (Wastell, 1977). Since we applied the latency-correction procedure to both prestimulus baseline and post-stimulus epochs, this effect would remove energy from the spectra of both. Thus, the values of Pearson's *r* should be free from effects due to "*locking on noise*".

Lange et al. (1997) used an alternative model of the evoked potential in which the amplitude and latency of each peak of the waveform is estimated on individual trials. This procedure would probably account for more variance in the data. However, as the number of parameters estimated for individual trials increases, the procedure would approximate a set of basic functions that could model any arbitrary waveform. In any event, more elaborate models of the evoked potential could be used. More complex models would make assumptions about the number of peaks to be modeled, or, for that matter, whether evoked potentials are more appropriately modeled as wavelets. The present study deals simply with the issue of amplitude and latency variability in the overall waveform.

Event-related desynchronizations found at 10 Hz and in the 20–30 Hz range are of particular interest since they are part of the unlocked component and represent dynamic brain activity underlying the attention related target conditions. We contend that this activity has largely gone undetected in most studies using the oddball paradigm that employed signal averaging in the time domain. Moreover, we also contend that ERD effects observed under these conditions would be expected, since they represent the disappearance of ongoing activity relative to baseline. This interpretation follows since an absent rhythm would not be expected to have any particular phase. Event-related desynchronizations have been described previously in the literature (e.g., Sergeant et al., 1987; Sutoh et al., 2000; Yordanova et al., 2001); however, the role of both stimulus-locked and unlocked components were not examined. Another interesting effect concerns the simultaneous ERD of the 4 Hz *unlocked* component to unattended standards and the ERS of the 4 Hz *stimulus-locked* component to unattended standards (Fig. 6). This reciprocal effect may represent stimulus-induced phase resetting, as suggested by Makeig et al. (2002). However, others suggest that when present, phase resetting may only be partial (Penny et al., 2002; Bogacz et al., 2002). Penny and colleagues have argued that phase resetting occurs only if the spontaneous background rhythm becomes synchronized to the stimulus with no overall change in energy. This appears to be the case in the 4 Hz stimulus-locked component shown in Fig. 6.

In those conditions that required attention to the target, EEG activity in the 1–2 Hz range was largely stimulus-locked and most prominent at the Pz electrode site. This could correspond to the well-known N100-P300 complex identified in time-domain averages, since modeling this complex waveform as a sinusoid would give a period around 400 ms (also see Kolev et al., 1997; Demiralp et al., 1999; Spencer and Polich, 1999; Yordanova et al., 2000). The unlocked component, most prominent at 4 Hz, represents a source of information *missing* from time-domain analyses. Since the regression procedure that was applied allowed for the assessment of relatively unlimited amplitude variability and considerable latency variability, it is probable that this component does *not* have a fixed waveform and therefore may reflect a transient dominance of energy in this frequency range. This microstate of EEG activity in the theta frequency range has been emphasized in the work of Yordanova et al. (2003), as being a basic process of stimulus evaluation present in response to both targets and non-targets. It is notable that Yordanova et al. (2003) applied wavelet decomposition to the averaged ERP. Consequently, their conclusions apply only to the stimulus-locked component. In contrast, our results show that it is the unlocked theta component that differentiates target from non-target conditions. Consistent with Yordanova et al. (2003), we also found that targets and non-targets could be differentiated by the stimulus-locked delta component. The importance of examining both components is suggested by the fact that the 4 Hz unlocked component has a different scalp topography than the stimulus-locked component and subsumes different reactivities of ongoing EEG to the effects of attention and stimulus conditions. These different scalp topographies may reflect different generators for locked and unlocked activity.

When EEG is used to study sensory, perceptual or cognitive processes, signal-processing strategies are dependent on the philosophical biases and theoretical orientation of the investigators. Use of spectral techniques allows for comparison of stimulus-locked and unlocked components of event-related activity. As suggested by Friston (2000) "*Transient coding subsumes both synchronous and asynchronous interactions and it is the later which mediate the nonlinear and context-sensitive features of brain dynamics*". Modeling evoked activity as spectral components emphasizes whole waveforms. This contrasts with the practice of associating specific cognitive processes to each peak or trough in the time-domain waveform (e.g. Luck et al., 2000). In a similar fashion, EEG oscillations at certain frequencies may be interpreted as corresponding to specific cognitive processes (e.g., Klimesch, 1999). Alternatively, low frequency oscillations may be associated with large populations of neurons responding in a synchronized manner, whereas high frequencies may be associated with smaller and more localized neuronal populations (e.g., Neuper and Pfurtscheller, 2001). This later interpretation does not necessarily ascribe a specific cognitive process to a specific frequency band, but rather, relates frequency bands of rhythmic activity to physical characteristics of the source. Whereas assigning relevance to specific time-domain peaks is consistent with linear-sequential models of information processing, emphasis on waveforms is more concordant with resonant models of information processing in the brain (e.g., Grossberg, 2000). The relative utility and implications of these different approaches remains to be determined.

5. Conclusions

A new regression based subtraction procedure is presented for extracting non-stimulus-locked event-related activity from individual trials of EEG. This signal processing strategy accounts for latency and amplitude variability in the stimulus-locked component and represents an improvement to the method proposed by Kalcher and Pfurtscheller (1995). Based on the oddball paradigm under active and passive listening conditions, it was found that a substantial amount of unlocked energy is retained in the event-related spectra after the stimulus-locked EEG component is removed. The unlocked activity was most evident during attention-related tasks involved in actively discriminating changes in stimulus frequency. Because unlocked activity is *not* detected in signal-processing strategies using time domain averaging, a substantial void exists in the available literature dealing with the processing of stimulus deviance. It is also shown that direct comparison of unlocked and stimulus-locked components provides new information about brain dynamics in response to sensory stimulation and cognitive activation. Nevertheless, much work needs to be done to further improve, validate and extend these observations and assertions.

Acknowledgements

Portions of this paper were presented at the annual meeting of the Association for Research in Otolaryngology, Daytona Beach, Florida, February 20003 and the Lake Ontario Hearing Meeting, University of Rochester, June 2003.

References

Başar, E., Bullock, T.H., 1992. Induced Rhythms in the Brain. Birkhäuser, Boston.

Bastiaansen, Hagoort, 2003. Event-induced theta responses as a window on the dynamics of memory. Cortex 39, 967–992.

Bogacz, R., Yeung, N., Holroyd, C.B., 2002. Detection of phase resetting in the electroencephalogram: an evaluation of methods. CD-ROM, Program No. 506.9, Society for Neuroscience, Washington, DC.

Buckner, R.L., Braver, T.S., 1999. Event-related functional MRI. In: Moonen, C.T.W., Bandettini, P.A. (Eds.), Functional MRI. Springer, New York, pp. 441–452.

Bullock, T.H., 1992. Introduction to induced rhythms: a widespread, heterogeneous class of oscillations. In: Başar, E., Bullock, T.H. (Eds.), Induced Rhythms in the Brain. Birkhäuser, Boston, pp. 1–26.

Cacace, A.T., McFarland, D.J., 2003. Spectral dynamics of electroencephalographic activity during auditory information processing. Hear. Res. 176, 25–41.

Dawson, G.D., 1951. A summating technique for detecting small signals in a large irregular background. J. Neurophysiol. 115, 2–3.

Dawson, G.D., 1954. A summation technique for the detection of small evoked potentials. Electroencephalogr. Clin. Neurophysiol. 6, 65–84.

Demiralp, T., Yordanova, J., Kolev, V., Ademoglu, A., Devim, M., Samar, V.J., 1999. Time-frequency analysis of single-sweep event-related potentials by means of fast wavelet transform. Brain Lang. 66, 129–145.

Donchin, E., Coles, M.G.H., 1988. Is the P300 component a manifestation of context updating? Behav. Brain Sci. 11, 357–374.

Friston, K.J., 2000. The labile brain. I. Neuronal transients and nonlinear coupling. Philos. Trans. R. Soc. Lond. B 355, 215–236.

Goncharova, I.I., McFarland, D.J., Vaughan, T.M., Wolpaw, J.R., 2003. EMG contamination of EEG: spectral and topographical characteristics. Clin. Neurophysiol. 114, 1580–1593.

Grossberg, S., 2000. The complementary brain: unifying brain dynamics and modularity. Trends Cogn. Sci. 4, 233–246.

Kalcher, J., Pfurtscheller, G., 1995. Discrimination between phase-locked and non-phase-locked event-related EEG activity. Electroencephalogr. Clin. Neurophysiol. 94, 381–384.

Klimesch, W., 1999. EEG alpha and theta oscillations reflect cognitive and memory performance: a review and analysis. Brain Res. Rev. 29, 169–195.

Klimesch, W., Russegger, H., Doppelmayr, M., Pachinger, T., 1998. A method for the calculation of induced band power: implications for the significance of brain oscillations. Electroencephalogr. Clin. Neurophysiol. 108, 123–130.

Kolev, V., Demiralp, T., Yardanova, J., Ademoglu, A., Isoglu-Alkac, U., 1997. Time-frequency analysis reveals multiple functional components during oddball P300. NeuroReport 8, 2061–2065.

Lange, D.H., Pratt, H., Inbar, G.F., 1997. Modeling and estimation of single evoked brain components. IEEE Trans. Biomed. Eng. 44, 791–799.

Luck, S.J., Woodman, G.F., Vogel, E.K., 2000. Event-related potential studies of attention. Trends Cogn. Sci. 4, 432–440.

Makeig, S., Westerfield, M., Jung, T.-P., Enghoff, S., Townsend, J., Courchesne, E., Sejnowski, T.J., 2002. Dynamic brain sources of visual evoked responses. Science 295, 690–694.

Melcher, J.R., Talavage, T.M., Harms, M.P., 1999. Functional MRI of the auditory system. In: Moonen, C.T.W., Bandettini, P.A. (Eds.), Functional MRI. Springer, New York, pp. 393–406.

Näätänen, R., 1992. Attention and Brain Function. Lawrence Erlbaum Associates, Hillsdale, NJ.

Näätänen, R., 2003. Mismatch negativity: clinical research and possible applications. Int. J. Psychophysiol. 48, 179–188.

Neuper, C., Pfurtscheller, G., 2001. Event-related dynamics of cortical rhythms: frequency-specific features and functional correlates. Int. J. Psychophysiol. 43, 41–58.

Nishida, S., Nakamura, M., Suwazono, S., Honda, M., Shibasaki, H., 1997. Estimate of physiological variability of peak latency in single sweep P300. Electroencephalogr. Clin. Neurophysiol. 104, 431–436.

Ohl, F.W., Deliano, M., Scheich, H., Freeman, W., 2003. Analysis of evoked and emergent patterns of stimulus-evoked auditory cortical activity. Rev. Neurosci. 14, 35–42.

Pfurtscheller, G., Lopes da Silva, F.H., 1999. Event-related EEG/MEG synchronization and desynchronization basic principles. Clin. Neurophysiol. 110, 1842–1857.

Penny, W., Kiebel, S.J., Kilner, J.M., Rugg, M.D., 2002. Event-related brain dynamics. Trends Neurosci. 25, 387–389.

Polich, J., Herbst, K.L., 2000. P300 as a clinical assay: rationale, evaluation, and findings. Int. J. Psychophys. 38, 3–19.

Press, W.H., Flannery, B.P., Teukolsky, S.A., Vetterling, W.T., 1988. Numerical Recipes in C: The Art of Scientific Computing. Cambridge University Press, New York.

Sergeant, J., Geuze, R., van Winsum, W., 1987. Event-related desynchronization and P300. Psychophysiology 24, 272–277.

Spencer, K.M., Polich, J., 1999. Poststimulus EEG spectral analysis and P300: attention, task, and probability. Psychophysiology 36, 220–232.

Sutoh, T., Yabe, H., Sato, Y., Hiruma, T., Kaneko, S., 2000. Event-related desynchronization during an auditory oddball task. Clin. Neurophysiol. 111, 858–862.

Truccolo, W.A., Ding, M., Knuth, K.H., Nakamura, R., Bressler, S.L., 2002. Trial-to-trial variability of cortical evoked responses: implications for the analysis of functional connectivity. Clin. Neurophysiol. 113, 206–226.

Wastell, D.G., 1977. Statistical detection of individual evoked responses: an evaluation of Woody's adaptive filter. Electroencephalogr. Clin. Neurophysiol. 42, 835–839.

Woody, C.D., 1967. Characterization of an adaptive filter for the analysis of variable latency neuroelectric signals. Med. Biol. Eng. 5, 539–553.

Yordanova, J., Devrim, M., Kolev, V., Ademoglu, A., Deiralp, T., 2000. Multiple time-frequency components account for the complex functional reactivity of P300. Neuroreport 11, 1097–1103.

Yordanova, J., Kolev, V., Polich, J., 2001. P300 and alpha event-related desynchronization (ERD). Psychophysiology 38, 143–152.

Yordanova, J., Rosso, J., Kolev, V., 2003. A transient dominance of theta event-related brain potential characterizes stimulus processing in an auditory oddball task. Clin. Neurophysiol. 114, 529–540.